ELSEVIER

Precambrian Research 69 (1994) 133–155

Precambrian Research

Palaeomagnetism and magnetic anisotropy of Proterozoic banded-iron formations and iron ores of the Hamersley Basin, Western Australia

P.W. Schmidt, D.A. Clark

CSIRO Division of Exploration and Mining, P.O. Box 136, North Ryde, N.S.W. 2113, Australia

Received July 21, 1992; revised version accepted January 27, 1994

Abstract

Rock magnetic properties and palaeomagnetism of weakly metamorphosed banded-iron formations (BIFs) of the Palaeoproterozoic Hamersley Group, Western Australia, and Proterozoic BIF-derived iron ores have been investigated. The BIF units sampled here are slightly younger than 2500 Ma. At Paraburdoo, Mount Tom Price and Mount Newman iron ore formation was completed before 1850 Ma.

Sampling was mainly from the Mount Tom Price and Paraburdoo mining areas and for the first time a palaeomagnetic fold test on fresh (unweathered and unaltered) BIF samples has allowed the nature of the remanence of the BIFs to be defined. The remanence of the BIFs is carried by late diagenetic/low-grade metamorphic magnetite after primary haematite. This remanence is pre-folding and is unlikely to be greatly affected by the high anisotropy because the palaeofield inclination was demonstrably low.

Determination of palaeofield directions from measured remanence directions is complicated by self-demagnetization effects in strongly magnetic, highly anisotropic BIF specimens. We present a method for correcting measured directions for the effects of self-demagnetization and anisotropy. For typical BIFs, the effect of magnetic anisotropy on measured remanence inclinations and inferred palaeolatitudes is minor for low palaeolatitudes, but can lead to large errors in calculated palaeopoles for intermediate to moderately steep palaeolatitudes. Anisotropy also causes cones of confidence to be underestimated, due to compression of the range of inclinations. In principle, deflection of post-folding remanence towards the bedding plane by high magnetic anisotropy can produce an apparent syn-folding signature, with best agreement between directions from different fold limbs after partial unfolding. Thus high anisotropy cannot only bias estimated palaeofield directions and cause underestimation of errors, but can also mislead interpretation of the time of remanence acquisition. The anisotropy of anhysteretic remanent magnetization (ARM) probably yields an upper limit to the anisotropy of the chemical remanent magnetization (CRM) carried by the BIFs. Therefore, from the anisotropy of ARM, a maximum inclination deflection of 9° is suggested for the sampled BIFs. This corresponds to less than 5° change of palaeolatitude.

The palaeomagnetic pole position calculated for BIFs at Paraburdoo is 40.9°S, 225.0°E ($dp=2.9°$, $dm=5.8°$) after tilt correction, but without correction for anisotropy. Other pole positions reported include that from flat-lying BIFs from Wittenoom at 36.4°S, 218.9°E ($dp=4.6°$, $dm=9.1°$), from Mount Tom Price iron ore at 37.4°S, 220.3°E ($dp=5.7°$, $dm=11.3°$) and from Paraburdoo ore at 36.4°S, 209.9°E ($dp=4.7°$, $dm=8.8°$). The poles from the BIFs, the Paraburdoo ore and the part of the Tom Price deposit that was sampled in this study are indistinguishable from each other and from the Mount Jope Volcanics overprint pole. The magnetization of the BIFs was probably acquired during burial metamorphism of the Hamersley Group, soon before the main folding and uplift event in the southern part of the Hamersley Province. This tectonic event exposed magnetite-rich BIFs

SSDI 0301-9268(94)00018-M

to near-surface oxidizing conditions, producing extensive martite–goethite orebodies and also appears to have produced the syn-folding overprint magnetization recorded by the Mount Jope Volcanics of the underlying Fortescue Group.

Ages of magnetization are tentatively interpreted as ~2200±100 Ma for the BIFs, ~2000±100 Ma for the supergene enrichment of BIF to martite–goethite ore, recorded by the Parabudoo and Mount Tom Price orebodies, and ~1950±100 Ma for the metamorphic martite–microplaty haematite ore, recorded as an overprint by the Tom Price orebody and as the only surviving magnetization of the Mount Newman orebody.

1. Introduction

This study of the magnetic properties and palaeomagnetism of the Hamersley Group, Western Australia (Fig. 1), extends the work of Schmidt and Embleton (1985) on the underlying Fortescue Group and basement terrane and was undertaken in collaboration with Australian exploration and mining companies under the auspices of AMIRA (Australian Minerals Industry Research Association). A knowledge of the remanent magnetization, the magnetic susceptibility and the anisotropy of magnetic susceptibility (AMS) of banded-iron formations (BIFs) and iron ores of the Hamersley Group was required to assist in exploration.

Previous palaeomagnetic work on the iron ores has been conducted by Porath and Chamalaun (1968), who showed that the ores probably formed in the Precambrian on the basis of their directions of remanent magnetizations, which were distinct from all known younger directions. The BIFs themselves were studied by Chamalaun and Dempsey (1978) and Embleton et al.

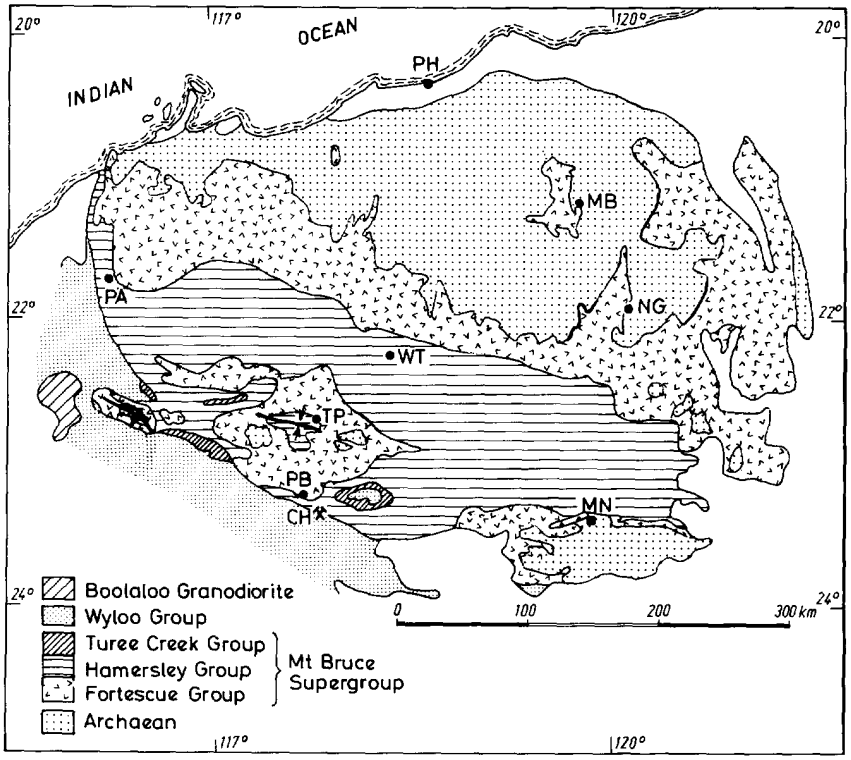

Fig. 1. Geological sketch map of the Hamersley Basin. *CH*=Channar; *MB*=Marble Bar; *MN*=Mount Newman (Whaleback); *NG*=Nullagine; *PA*=Pannawonica; *PB*=Paraburdoo; *PH*=Port Hedland; *TP*=Mount Tom Price; *WT*=Wittenoom.

(1979) who found surface samples to be badly affected by weathering and/or lightning. However, these latter workers were able to isolate a stable ancient magnetic direction from oriented drill core although the lack of a fold test precluded assigning a relative age to the magnetization.

2. Geology and sampling

The Mount Bruce Supergroup unconformably overlies the Archaean granite/greenstone basement terrane of the Pilbara Craton and is comprised of three distinctive, but essentially conformable, groups. In ascending order these are: the Fortescue Group (predominantly volcanic sequences), the Hamersley Group (chemical sediments) and the Turee Creek Group (predominantly clastic sediments). The Mount Bruce Supergroup is unconformably overlain by the Lower Wyloo Group, which in turn is unconformably overlain by the Upper Wyloo Group. A zircon U–Pb age of 2925 ± 16 Ma has been obtained from the Munni Munni Complex of the basement terrane (Arndt et al., 1991) while a zircon U–Pb age of 1843 ± 2 Ma has been obtained from the June Hill Volcanics of the Upper Wyloo Group (Pidgeon and Horwitz, 1991). The intrusion of the Wyloo Group by a post-tectonic granitoid, the Boolaloo Granodiorite, dated at 1684 Ma (Leggo et al., 1965), places an upper age limit to the deformation of the Hamersley Basin, although it should be noted that the Mount Bruce Supergroup was already deformed to some extent before deposition of the unconformably overlying Wyloo Group, i.e. before 1843 Ma. Other geochronological constraints on the evolution of the Hamersley Basin have been summarized by Trendall (1983, 1990). The stratigraphy and evolution of the Hamersley Basin are summarized in Fig. 2.

The 2.5 km thick Hamersley Group comprises five major and several minor banded-iron formations (BIFs) separated by shales and dolomites, with a prominent extrusive and intrusive unit, the Woongarra Volcanics, intercalated between the two uppermost BIFs (Trendall and Blockley, 1970). In ascending order the major BIFs are: the Marra Mamba Iron Formation, the Brockman Iron Formation (which is sub-divided into the Dales Gorge Member and the Joffre Member), the Weeli Wolli Formation and the Boolgeeda Iron Formation. The Wittenoom Dolomite occurs between the lowest two BIFs. The BIFs are remarkable in that they can be correlated practically across the whole basin, covering an area of about 100,000 km^2. In one of the BIF units, the Dales Gorge Member, even small-scale (few centimetres) banding can be correlated basin-wide (Trendall and Blockley, 1970; Ewers and Morris, 1981).

The iron ores of the Hamersley Basin are of many types and ages and have been derived, either directly or indirectly, from the BIFs. The youngest ores are the haematite conglomerates ("canga") and the pisolitic goethitic–haematitic ores, which are of late Mesozoic and Tertiary origin. Much older, however, are the giant microplaty haematite BIF-hosted iron ores. These represent the largest and most mature ores in the province and have been studied by many workers, as summarized by Morris (1983, 1985), Blockley (1990) and Harmsworth et al. (1990).

The myriad of mineralogical and textural varieties present in the ores has been studied in detail by Morris (1980, 1985). The following brief summary of current ideas on the BIF to ore transformation is far from comprehensive and only serves to give the reader a flavour of the complex evolution recognized by Morris. Following exposure of fresh BIF during a period of uplift and erosion, iron has been concentrated at depth by an electrochemical supergene process. This involved concentration by leaching of some gangue without replacement, as well as the metasomatic replacement of gangue (chert and carbonates) by hydrous iron oxides, mostly goethite. The iron in this metasomatic goethite is derived from weathering of BIF up-dip from the zone of ore formation. Magnetite in the fresh BIF is converted to martite and cation-deficient magnetite, termed "kenomagnetite" by Morris (1980, 1985), during the ore-forming process. In areas of favourable structure, these effects penetrated deeply enough to have avoided later ero-

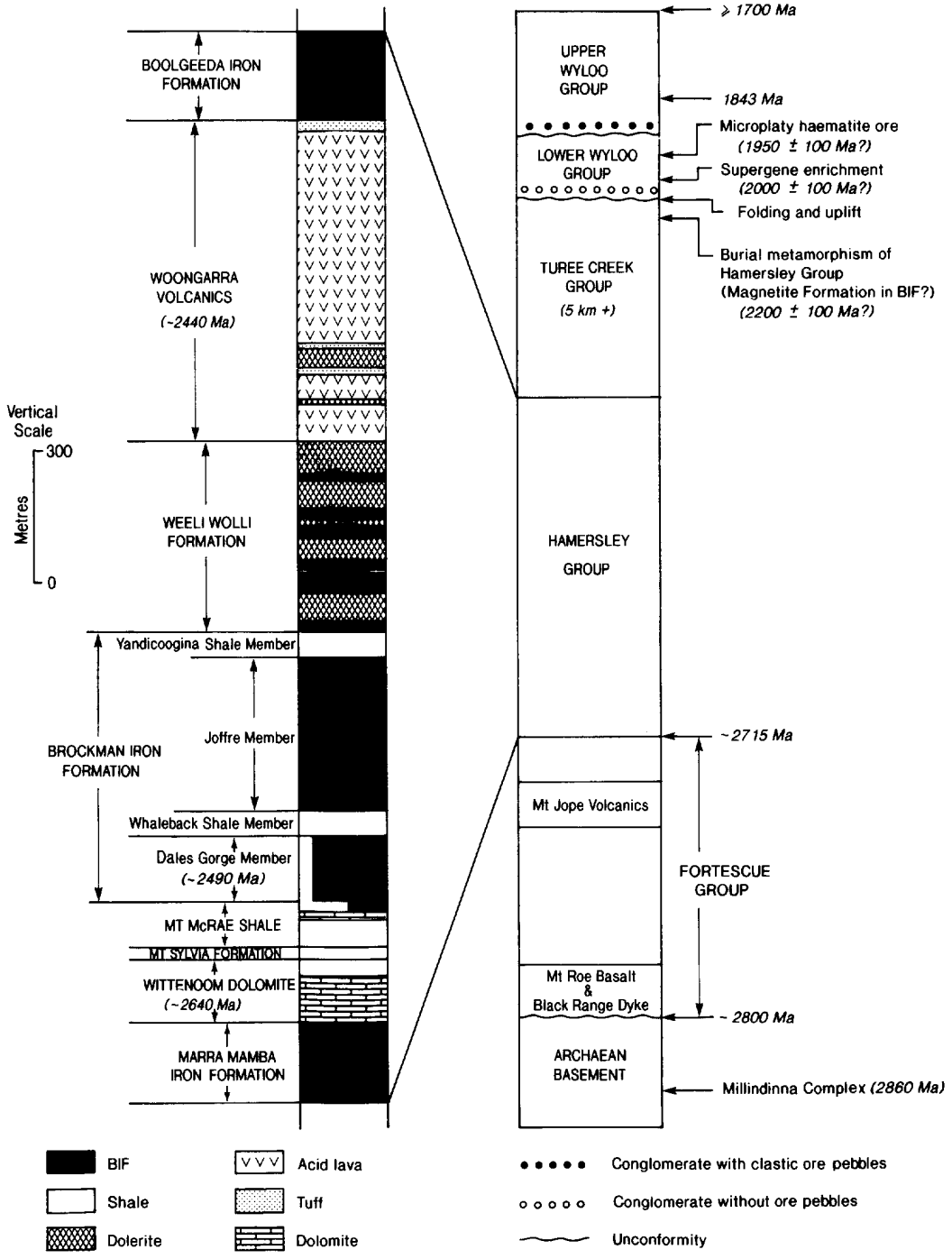

Fig. 2. Stratigraphy and key geological events of the Hamersley Basin, including detailed stratigraphy of the Hamersley Group.

sion. The hydrated iron oxides were largely converted to haematite with a characteristic microplaty habit at temperatures of ~100°C during subsequent burial of the martite–goethite ores. Later exhumation of the resulting martite–microplaty haematite-residual goethite ores can lead to significant economic upgrading due to leaching of goethite by circulating groundwaters. The ores at Mount Tom Price (TP) and Mount Newman (MN) represent those that have undergone this upgrading following uplift in the Mesozoic or Tertiary, while the process at Paraburdoo (PB) appears to have been arrested before this final stage and the ore still contains goethite (Fig. 1). The ores are characterized by a condensed stratigraphy and moderate deformation resulting from a large volume decrease (up to 50%) from fresh BIF to ore. Horwitz (1983) has related the high-grade ores to the margins of the Precambrian McGrath Trough, supporting the proposition of the importance of surface exposure and supergene enrichment in the initiation of these ores.

The Hamersley BIFs above the Wittenoom Dolomite are thought to be slightly younger than 2500 Ma. Zircon ages of 2490 ± 20 Ma have been reported from the Dales Gorge Member (Compston et al., 1981) and of 2439 ± 10 Ma from the stratigraphically higher Woongarra Volcanics (Pidgeon and Horwitz, 1991). The lowest of the BIFs, the Marra Mamba Iron Formation, may be much older than the upper BIFs, perhaps closer in age to the underlying Fortescue Volcanics (from 2765 Ma to 2715 Ma according to zircon U–Pb ages from Arndt et al., 1991), since a zircon U–Pb age of approximately 2640 ± 20 Ma has been derived from the Wittenoom Dolomite (Hassler, 1993). There is no sign of an unconformity or disconformity between the Wittenoom Dolomite and overlying Brockman Iron Formation; indeed, depositional conditions at the time were extraordinarily stable.

The Hamersley and Fortescue Groups were subjected to low-grade (lowermost prehnite–pumpellyite facies to lowermost greenschist facies) metamorphism due to burial beneath ⩾5 km of the Turee Creek Group (Smith et al., 1982), before the initial folding, uplift and partial erosion of the Mount Bruce Supergroup. Metamorphic temperatures in the Hamersley Group nowhere exceeded ~300°C and are often considerably lower. A slightly lower grade of burial metamorphism at Paraburdoo is associated with relict primary haematite overgrown by magnetite in the BIFs, whereas elsewhere, e.g. at Mount Tom Price and Wittenoom, the metamorphic grade is higher and replacement of primary haematite by magnetite is essentially complete (Morris, 1985). This is evidence that most of the magnetite in the BIFs was produced during the burial metamorphism. Klein (1983) has discussed diagenesis and metamorphism of BIF, including the generation of magnetite as a late diagenetic/low-grade metamorphic mineral.

It has been suggested that the change from the "anoxic" conditions conducive to BIF formation, to those favouring supergene iron enrichment, was related to the oxygen content of the Precambrian atmosphere reaching a threshold level able to satisfy the various oxygen "sinks" (Cloud, 1983). This is thought to have been attained through photosynthesis from 2300 Ma to 2000 Ma, based on the first appearance of red beds in the geological record. Stratigraphic evidence from the Hamersley Basin constrains initiation of ore formation to the period of deposition of the overlying Wyloo Group. In particular, two conglomerates have been recorded within the Wyloo Group, the lower one contains only BIF clasts, while the upper one contains both BIF and ore clasts, suggesting that at least some ore formed in the period of time separating their deposition. The overlying June Hill Volcanics of the Upper Wyloo Group thus constrain the initiation of ore formation to be older than 1843 ± 2 Ma (Pidgeon and Horwitz, 1991). Morris (1985) has suggested an age of about 2000 Ma for the initial ore formation, which is consistent with this recent age determination, and has correlated similar BIF-hosted iron ores in other continents, without violating known age constraints.

The sites sampled for this project lie in the Tom Price and Paraburdoo mining areas of the Hamersley Basin, Western Australia (Fig. 1). The iron ores present at these places are of the high-grade

microplaty haematite type, although the Paraburdoo ore is slightly less mature than the Tom Price ore in that the final leaching of goethite did not occur at Paraburdoo. This is possibly related to structures resulting from the intrusion of pre-ore dolerites and to modified hydrologic conditions at Paraburdoo (Morris, 1980).

Forty-two independently oriented block samples and fifteen drill core samples were collected from the Tom Price area, while thirty block samples and eighteen drill core samples were collected from the Paraburdoo area. Apart from samples of ore collected in the open-cut mines, other samples included those from oxidized BIFs from the Tom Price area, those from the conglomerate containing ore clasts in the overlying Wyloo Formation at Paraburdoo and unoriented samples from surficial deposits, Channar ore and "canga", also from the Paraburdoo area. Results from fresh Wittenoom BIF cores (Dales Gorge and Joffre Members) reported by Embleton et al. (1979) and previously unpublished results from three oriented samples of ore from Mount Newman (MN in Fig. 1), have also been incorporated in this study.

3. Methods and techniques

Standard palaeomagnetic procedures (Collinson, 1983) were followed throughout this study. Block samples were oriented using both a sun compass and a magnetic compass, and while the drill core samples from Tom Price were not azimuthally oriented, those from Paraburdoo could be oriented using the very consistent bedding attitude present at this locality. The blocks and cores were sub-sampled in the laboratory to yield specimens of nominal 25 mm diameter and 20 mm height. Remanent magnetizations were measured using a CTF cryogenic magnetometer or an up-graded DIGICO balanced fluxgate magnetometer. The spinner unit and electronic drive unit of the latter have been interfaced to a personal computer.

The CSIRO susceptibility bridge/furnace (Ridley and Brown, 1980) was used to measure absolute susceptibilities and to monitor susceptibility variations with temperature (k–T). The apparent susceptibility of strongly magnetic specimens is affected by self-demagnetization. Based on analysis of the reluctance of the magnetic circuit comprising the toroidal transformer-steel core, the gap in the core and the specimen within the gap, the effective SI demagnetizing factor for the bridge is equal to:

(length of gap
−length of specimen)/length of gap = 0.13

True susceptibilities (k_{zz}) along the axis of the specimens were calculated from the apparent susceptibilities (k'_{zz}) using this demagnetizing factor, i.e.:

$$k_{zz} = k'_{zz}/(1 - 0.13k'_{zz})$$

Anisotropy of magnetic susceptibility was determined using an up-graded DIGICO anisotropy delineator whose performance exceeds that of the original. This has been calibrated against the susceptibility bridge, avoiding the calibration problem brought to light by Hrouda et al. (1983) and Veitch et al. (1983). The alternative coil set provided with the anisotropy delineator for high-susceptibility specimens was used for strongly magnetic BIF samples. In this configuration the applied field is produced by a large Helmholtz coil set and the coils that normally provide the applied field are used for detection of the anisotropy signal, rather than the smaller pick-up coils, which are close to the specimen in order to maximize sensitivity when measuring weakly magnetic specimens. This configuration minimizes the effects of inhomogeneity of field and magnetization for high susceptibilities, when self-demagnetization becomes important.

This instrument measures changes in susceptibilities along different directions, rather than absolute susceptibilities, which are measured independently on the susceptibility bridge. The apparent susceptibility differences are reduced with respect to the intrinsic susceptibility differences by self-demagnetization of the quasispherical specimens, for which the SI demagnetizing factor is 1/3. The "bulk susceptibility" (the apparent susceptibility along the specimen z-axis) used

to calculate principal susceptibilities and anisotropy ratios was:

$k_{zz}/(1+k_{zz}/3)$

The intrinsic susceptibility tensor of the specimen can then be calculated from the measured susceptibility tensor by inverting the self-demagnetization correction.

Alternating field (AF) demagnetization was carried out by means of the CSIRO three-axis tumbler, similar to that described by Roy et al. (1973), or a Schonstedt GSD-1 demagnetizer. The CSIRO programmable carousel furnace, which allows multiple batches of samples to be processed unattended, was used for stepwise thermal demagnetization. Linearity spectrum analysis (LSA, Schmidt, 1982) was used to identify linear segments for groups of specimens from the same site, formation or drill core.

4. Rock magnetism

4.1. Low-field thermomagnetic curves

Thermomagnetic analyses of representative samples of different lithologies were carried out in order to identify the magnetic minerals present and to estimate their relative contributions to the magnetic properties of the rocks and ores. The susceptibilities of small crushed sub-samples were continuously monitored as a function of temperature between −196°C and 700°C. The resulting k–T curves are shown in Fig. 3.

Fresh BIF from Paraburdoo (e.g. sample 42/300.5) yields a "type" curve for multidomain stoichiometric magnetite with a prominent isotropic point at around −155°C, and a Curie point of 580°C. The reversibility of the curve indicates that the chemical changes during the heating are negligible, and that only magnetic transitions are observed.

The behaviour of a sample of Mount Newman ore (MN01B) is much more complicated but is nevertheless readily interpretable. The susceptibility of unheated ore at ambient temperature is due, in approximately equal measure, to haematite and to fine-grained magnetite or cation-deficient (CD) magnetite. Because of its much higher specific susceptibility, magnetite sensu lato is much less important volumetrically. Petrographic studies of Mount Newman ore indicate the presence of minor secondary CD magnetite, resulting from reduction of haematite, within the martite ore (R.C. Morris, pers. commun., 1992). At the Morin transition there is an increase in total susceptibility due to the appearance of weak ferromagnetism in haematite. Above 400°C there is a spectacular unblocking peak associated with fine-grained CD magnetite. The form of this k–T curve is consistent with a very restricted grain size distribution for the CD magnetite, within the single domain size range. The contribution due to CD magnetite vanishes above ~600°C, just above the Curie point of stoichiometric magnetite, leaving the contribution of haematite, which in turn disappears at 680°C. The irreversibility of this k–T curve on cooling indicates that chemical changes have taken place at high temperatures, with the production of extra (CD) magnetite approximately doubling the original (very small) fraction of CD magnetite in the sample.

Oxidized Dales Gorge BIF (TP01B) from the Synclines Deposit, Tom Price is also interpreted in terms of a mixture of haematite and magnetite. In this case the magnetite is more coarse-grained than in the Mount Newman ore sample, as evidenced by the isotropic point, and the lack of an unblocking peak at high temperatures. The susceptibility peak at the isotropic point is diagnostic of stoichiometric, or very slightly cation-deficient, magnetite. The irreversibility of the curve (smaller signal on cooling) shows that some magnetite and haematite have been destroyed by heating. The non-magnetic phases that must have been created are not known.

The magnetic ore from the Channar deposit has a fully reversible k–T curve which clearly indicates that the magnetic properties are dominated by a small fraction of multidomain nearly stoichiometric magnetite (note the isotropic point and the relatively flat curve up to the magnetite Curie point). Approximately 4% of the room-temperature susceptibility is contributed by the volumetrically dominant but weakly mag-

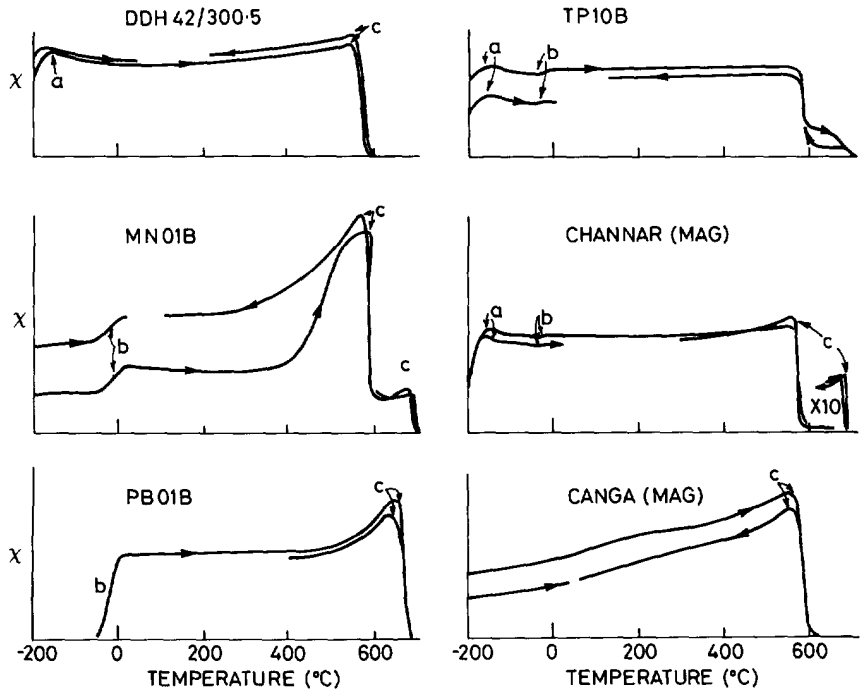

Fig. 3. Susceptibility versus temperature for different iron ores and banded-iron formations (BIFs). *DDH42/300.5* = BIF from 300.5 m depth in drill hole 42 at Paraburdoo; *TP10B* = from Mount Tom Price martite–microplaty haematite ore; *MN01B* = from Mount Newman martite–microplaty haematite ore; *Channar (MAG)* = a (contact) metamorphosed microplaty haematite–goethite ore with minor magnetite; *PB* = from martite–microplaty haematite–goethite ore from Paraburdoo; and *Canga (MAG)* = from a haematite ore enriched through weathering. (*a* = isotropic point; *b* = Morin transition; *c* = Curie point.)

netic microplaty haematite. The magnetite in Channar ore is secondary and was produced during contact metamorphism associated with a large dolerite dyke.

Unlike the BIF at Paraburdoo, our ore samples from the mine contain no magnetite (e.g. PB01B). The reversible *k–T* curve exhibits a sudden rise in susceptibility, from a very low value, at the Morin transition and a Curie temperature of 680°C. The Hopkinson peak indicates unblocking temperatures in the approximate range 500–650°C, suggesting that this ore should be a reliable palaeomagnetic recorder.

The magnetic canga sample exhibits a steady increase of susceptibility with temperatures from −196°C up to ~580°C, with a Curie point just above 600°C. There is no sign of an isotropic point. This type of *k–T* curve typifies weathered profiles containing fine-grained CD magnetite. The wide spectrum of unblocking temperatures indicates the presence of a grain size fraction that is superparamagnetic (SPM) at ambient temperatures. Magnetic canga typically contains remnant cores of CD magnetite, as well as secondary CD magnetite formed from hydrous iron oxides during weathering (R.C. Morris, pers. commun., 1992). A sample of relatively weakly magnetic canga was shown to contain a lower proportion of multidomain stoichiometric magnetite, with a perceptible contribution to the susceptibility from a volumetrically dominant proportion of haematite.

4.2. Anisotropy of magnetic susceptibility (AMS)

The anisotropy of the BIFs was found to be strong, and therefore could be important to the determination of the palaeofield direction. The directions of the principal axes of the anisotropy ellipsoids strongly reflect the banding in the BIF

(corresponding to the palaeohorizontal), with the maximum and intermediate axes constrained to the plane of the banding and the minimum axis perpendicular to the banding.

Overall the susceptibilities and the AMS of all the BIFs seem to be fairly similar. The intrinsic (true as opposed to apparent) susceptibility parallel to bedding probably lies in the range 0.63–1.3 SI (0.05–0.1 G/Oe) in most localities, with an intrinsic anisotropy of 2–4. Bearing in mind that these values pertain to extensive beds, and not short cylindrical palaeomagnetic specimens, this nevertheless suggests that any observed remanent magnetizations in the BIF samples may be deflected towards the bedding plane, away from the palaeofield direction. This is taken into account in the discussion below on the remanent magnetization.

5. Palaeomagnetism

5.1. *In-situ remanent magnetizations*

Previous studies (Chamalaun and Dempsey, 1978; Embleton et al., 1979) have shown that the remanence carried by outcropping Hamersley BIF units is very complex and difficult to interpret. Generally, it appears to be weathering and/or lightning that has affected surface exposures and it has proved necessary to concentrate on diamond-drill core samples. The orientation of the drill core samples is possible using the available drill hole survey data in conjunction with either a consistently oriented basin-wide asymmetric crenulation in the BIF (A.F. Trendall, pers. commun., 1976) or a consistent bedding attitude. These new results from dipping BIF units augment the earlier drill core results from flat-lying BIFs at Wittenoom (Embleton et al., 1979).

Many of the samples collected from outcrops have NRM directions that are highly divergent from the characteristic direction for the area, and some of these exhibit extremely high Koenigsberger (1938) ratios (Q). Such magnetizations are almost certainly lightning-induced. In some areas, combined AF and thermal demagnetization has been shown to be very effective when dealing with rocks whose remanences have been disturbed by relatively strong magnetic fields (>5 mT) such as those accompanying lightning strikes (Schmidt and Embleton, 1985). Although this approach was adopted here as a routine procedure for treating samples collected from natural outcrop, samples from natural outcrops often yielded scattered remanence directions after treatment.

The remaining outcrop samples appear to have escaped significant IRM overprinting and their NRM directions may be regarded as representative of oxidized BIF. Moderate weathering of BIF should reduce both the susceptibility and remanence as magnetite alters to haematite. However, remanence direction should remain unchanged as long as even a small fraction of unoxidized magnetite remains to dominate the NRM. Eventually, complete oxidation of the magnetite should produce weak NRMs similar to those of Tertiary laterites with scattered normal and reversed groups, plus many intermediate directions (see Schmidt and Embleton, 1976; Idnurm and Senior, 1978; Idnurm and Schmidt, 1986).

5.2. *Paraburdoo results*

Representative demagnetization behaviour for surface samples, mainly iron ore and oxidized BIF, from Paraburdoo is displayed as orthogonal projections (Zijderveld, 1967) in Fig. 4. All these samples were collected from the mine, except for those from the conglomerate of the Mount McGrath Formation. Both directions and intensities of most samples are very stable and the magnetizations only decrease significantly after heating to 600–670°C, i.e. between the Curie points of magnetite and haematite, and disappear finally just below the Curie point of haematite. This indicates that haematite with high unblocking temperatures is the main remanence carrier in these samples. Typically, samples show a single component of magnetization (Figs. 4a–4e), although one sample (Fig. 4f) reveals multicomponent magnetization. The latter type of complicated magnetic signature is found in all samples of the Mount McGrath Formation con-

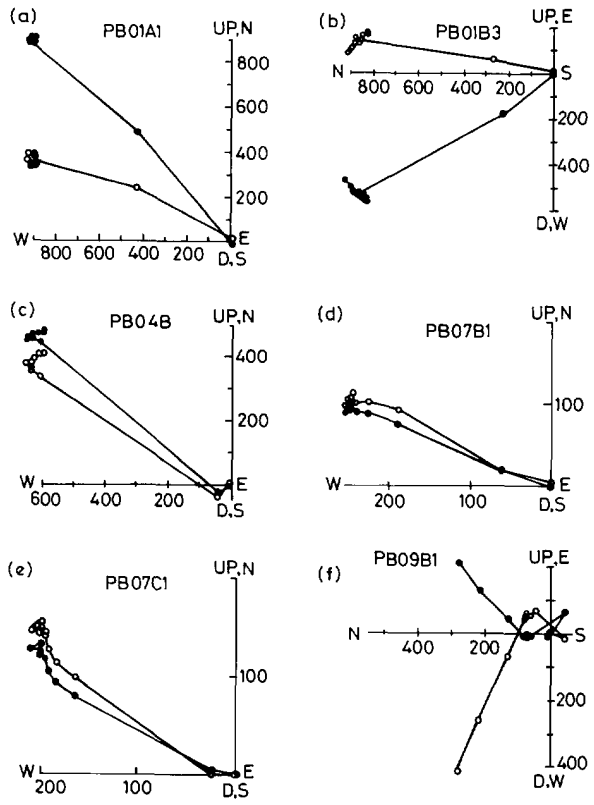

Fig. 4. Orthogonal projections of AF and thermal demagnetization of Paraburdoo iron ore samples. Demagnetization steps following NRM are 1 mT, 5 mT, 10 mT, 20 mT, 30 mT, 200°C, 300°C, 400°C, 500°C, 600°C, 670°C and 690°C. Units are in mA m^{-1}.

glomerate, and since these samples possess very high Koenigsberger ratios, and there is no consistency of direction between clasts, lightning is probably the cause. We note, however, that the result could be interpreted naively in terms of a conglomerate test (Graham, 1949), suggesting that the magnetic components of the individual ore clasts predate deposition of the conglomerate. Other samples that display aberrant behaviour came from sites that were weathered and/or lightning-affected and are not considered further.

NRMs of BIF drill core samples, and most of the ore samples from operating mines, consist essentially of stable ancient components, that are directed northwest and have negative inclinations, overprinted to varying degrees by soft components with no consistent orientation. These soft components are attributed to post-sampling effects, e.g. isothermal remanent magnetization (IRM) imparted during core logging using hand magnets. With few exceptions, there is little evidence of a significant viscous remanent magnetization (VRM) component in the samples, including those samples not contaminated with contemporary IRM noise. Most of the divergence in NRM directions in drill core samples was removed in fairly low AFs (5–10 mT), within the range of values of small permanent magnets. Orthogonal projections of the demagnetization of remanence vectors from Paraburdoo diamond-drill hole (DDH) samples are presented in Fig. 5, where both AF and thermal demagnetizations are compared. For some oxidized BIFs, e.g. sample (DDH44)49.8 from the Weeli Wolli Formation, complete demagnetization is achieved only after thermal demagnetization to about 690°C. In duplicate specimens from the same sample, magnetization directions after AF cleaning to 100 mT are similar to those of their thermally demagnetized counterparts, although the AF-cleaned specimens are not fully demagnetized (Figs. 5a and 5b). The results from sample (DDH42)207.0 demonstrate the efficacy of AF demagnetization in selectively destroying spurious IRM components, as compared to thermal demagnetization. On thermal demagnetization some specimens attained a stable magnetic direction only at high temperatures (Fig. 5c), but for duplicate specimens, a single AF step of 5 mT (Fig. 5e) swings the remanence direction through a large angle which remains essentially stable on further thermal demagnetization (Fig. 5f). However, it is apparent that both techniques yield similar results. Directions from the Marra Mamba Formation were scattered and are thought to reflect the heavily weathered state of the samples.

Stereographic projections of NRM and cleaned directions from the fresh BIF are shown in Fig. 6. The NRMs from DDH44 are mainly clustered in the northwest up octant, while those from DDH42 show a spread of directions in the bedding plane (Fig. 6a). However, after cleaning all

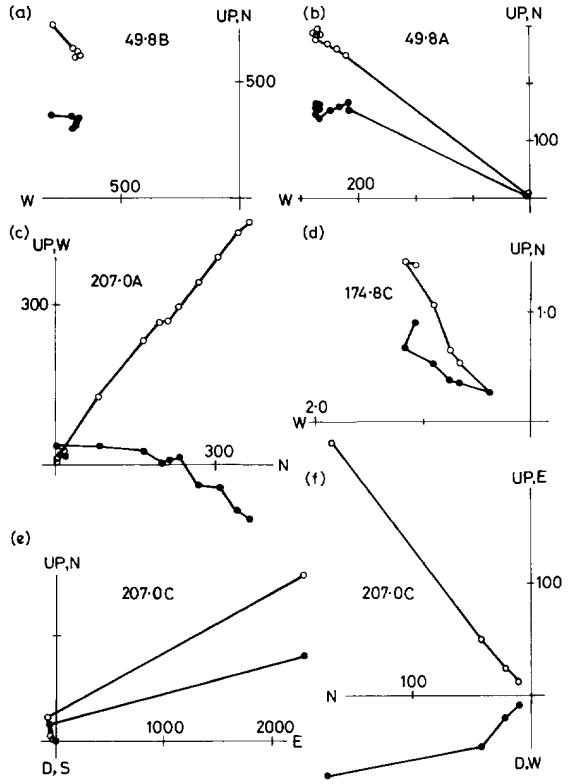

Fig. 5. Orthogonal projections comparing AF and thermal demagnetization of Paraburdoo banded-iron formation samples. (a) AF only to 100 mT; (b) AF and thermal as for Fig. 4; (c) thermal only as for Fig. 4; (d) AF only to 100 mT; (e) AF and thermal as for Fig. 4; and (f) enlargement of (e). Units are in mA m^{-1}.

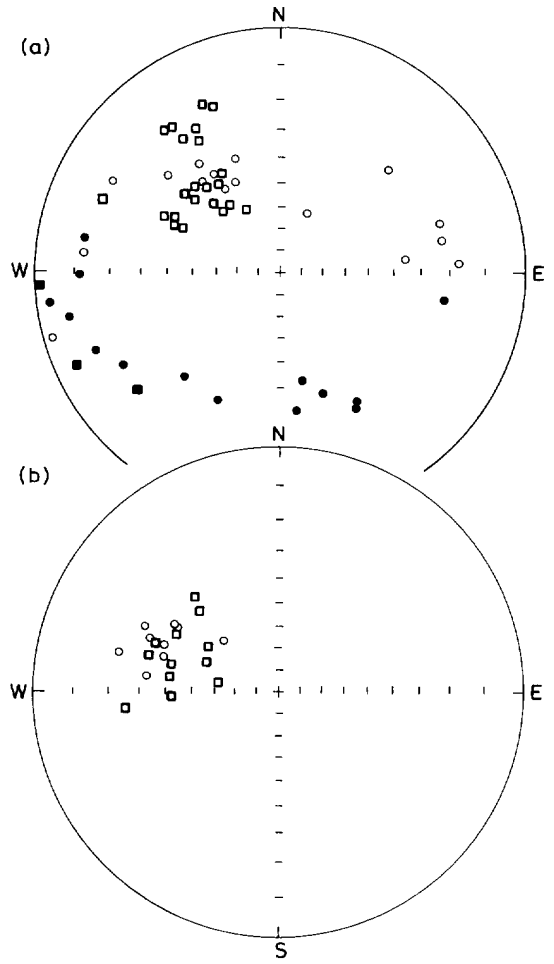

Fig. 6. Equal-angle stereonet showing: (a) natural remanent magnetization directions; and (b) cleaned remanent magnetization directions for banded-iron formation samples from Paraburdoo. Circles represent samples of DDH42 while squares represent samples from DDH44. Note the scatter of NRM directions in the south-dipping bedding plane (not corrected for tilt or anisotropy). Closed (open) symbols down (up).

directions converge to the upper northwest octant (Fig. 6b).

5.3. Tom Price results

The orthogonal projections of Fig. 7 show representative demagnetization behaviour of surface samples (iron ore and oxidized BIF) from Tom Price. These samples are not as stable as those from Paraburdoo, although they are still very stable. The main difference between the Paraburdoo and Tom Price samples is that the latter possess a broad spectrum of unblocking temperatures as opposed to the narrow, or discrete, unblocking temperatures displayed by the Paraburdoo samples. Most remanence vectors are directed northwest and up, although one specimen (TP05B1) is magnetized in the southeast and up direction, suggesting the presence of opposite polarities of remanence (Fig. 7c). On closer inspection it is apparent that the demagnetization trajectory of this specimen is not approaching the origin, but is heading towards the northwest/up octant. Much of the scatter of NRM directions of samples from the Tom Price

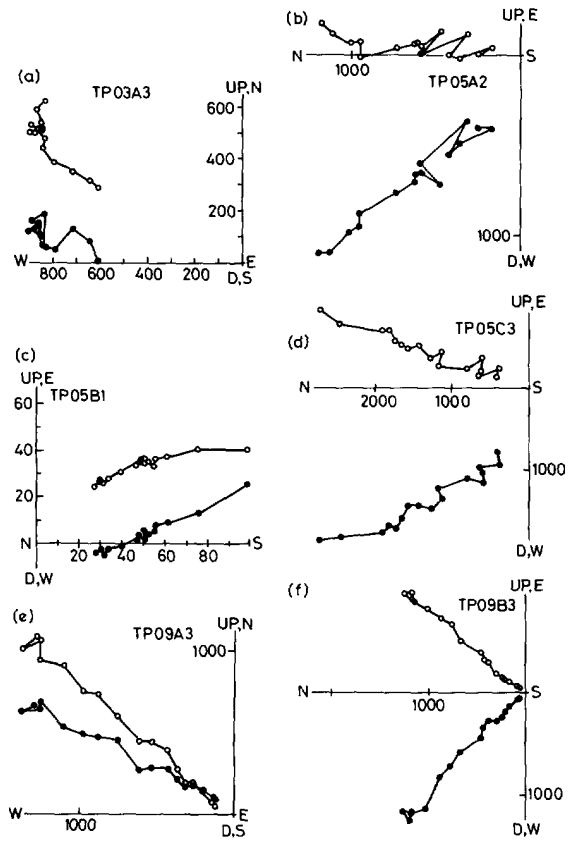

Fig. 7. Orthogonal projections for AF+thermal demagnetization of Mount Tom Price iron ore samples. Demagnetization steps following NRM are 5 mT, 10 mT, (20 mT), 200°C, 300°C, 350°C, 400°C, 450°C, 500°C, 530°C, 570°C, 580°C, 600°C, 630°C, 660°C and 670°C. Units are in mA m^{-1}.

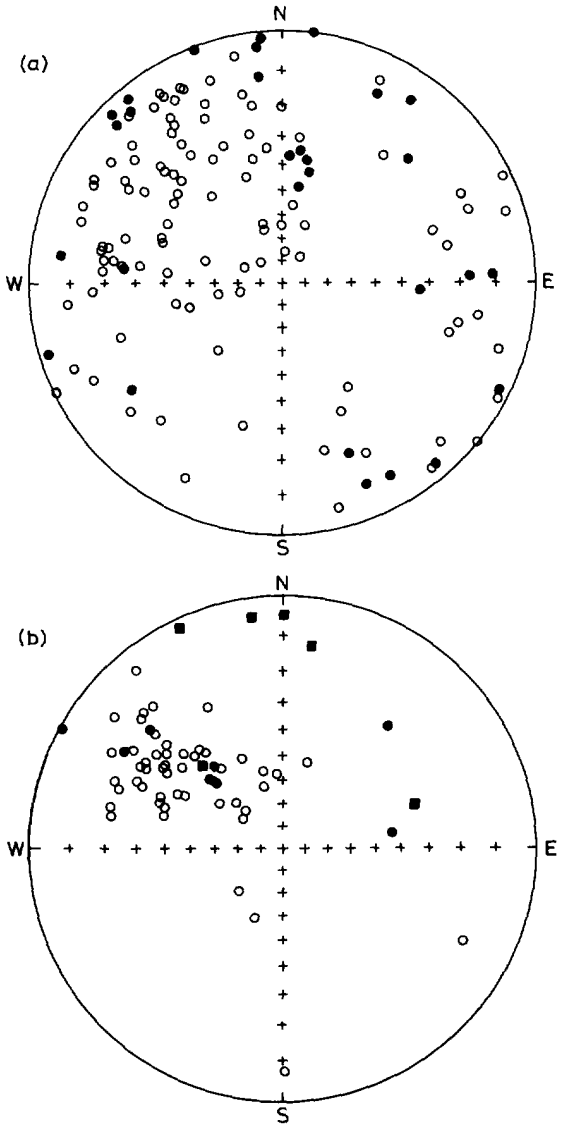

Fig. 8. Equal-angle stereonet showing: (a) natural remanent magnetization directions from iron ore and oxidized BIF from Mount Tom Price; and (b) natural remanent magnetization directions from iron ore and oxidized BIF from Paraburdoo, including samples of iron ore clasts from the Mount McGrath Formation conglomerate plotted as squares. Conventions as for Fig. 6.

mine probably arises from the coexistence of both magnetic polarities within single specimens.

The NRM directions of all specimens collected from the mine and natural outcrops are displayed in Fig. 8a for Mount Tom Price and Fig. 8b for Paraburdoo. Although directions are scattered (particularly those from Tom Price, reflecting the contribution of samples from elevated areas around Mount Nameless), there is nevertheless a clear tendency to group in the upper northwest octant, similar to the grouping of directions for the fresh BIF at Paraburdoo. Results from the samples of natural outcrops near Tom Price are most readily explained as the con-

sequence of lightning and are not considered further.

5.4. Tilt correction of BIF cleaned remanent magnetizations

The in-situ NRM directions for BIF samples from both Wittenoom and Paraburdoo are plotted in Fig. 9a. After correction for simple tilt of the bedding, the cleaned directions of magnetization from the BIFs are found to converge in the northwest quadrant, giving a mean direction of shallow negative inclination, i.e. slightly upward (Fig. 9b). Table 1 lists the mean directions before and after tilt correction. Applying the fold test of McFadden and Jones (1981), a common true mean direction for the Wittenoom and Paraburdoo BIFs is rejected with more than 99% confidence before tilt correction, but cannot be rejected, even with only 86% confidence, after tilt-correction. This therefore constitutes a positive fold test and indicates that the BIFs acquired their magnetization before folding. The fold test assumes, however, that the directions are Fisher distributed, which is not the case here because the distribution of inclinations has been somewhat compressed by the anisotropy. In principle, therefore, the fold test is only qualitative. Nevertheless, it is obvious on inspection of the distributions of directions that the populations from each limb are inconsistent before tilt correction and are completely overlapped after full tilt correction, with no indication of crossover of mean directions for partial tilt correction. Thus the data clearly support the interpretation that the characteristic remanence is prefolding, although rigorous confidence limits cannot be calculated.

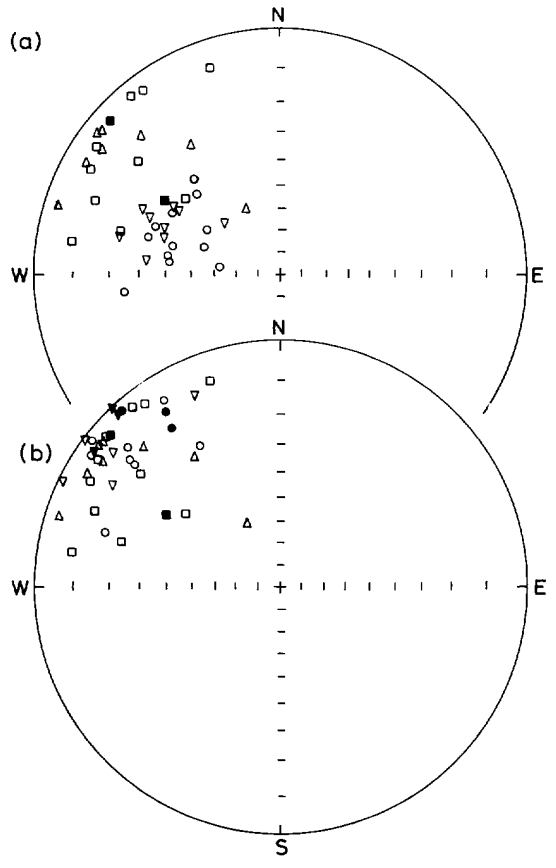

Fig. 9. Equal-angle stereonet showing: (a) in-situ cleaned remanent magnetization directions from BIF samples from Paraburdoo (inverted triangles DDH42, Dales Gorge Member and circles DDH44, Weeli Wolli and Joffre Members) and Wittenoom (squares DDH51, Dales Gorge Member and upright triangle DDH47A, Joffre Member); and (b) cleaned remanent magnetization directions for same samples corrected for bedding tilt of about 60° to the south at Paraburdoo. Conventions as for Fig. 6.

The positive fold test suggests that the remanence carried by the BIFs is a chemical remanent magnetization (CRM) acquired during crystallization of the magnetite. The characteristically high unblocking temperatures of the magnetite imply that thermal overprinting of the CRM by the very low-grade metamorphism experienced by the Hamersley Group should be negligible. The remanence of the BIFs is essentially monocomponent (except for some IRM noise without geological significance), in accord with this supposition. We therefore interpret the characteristic magnetization of the BIFs as acquired during formation of the magnetite, i.e. during late diagenesis or burial metamorphism, but before deformation of the Hamersley Group in latest Turee Group time or earliest Wyloo time.

In principle, the measured inclinations should be corrected for the anisotropy of the BIF specimens. This is discussed in detail in the next sec-

Table 1
Summary of magnetization directions after cleaning

Unit	N	D_h (°)	I_h (°)	α_{95} (°)	D_b (°)	I_b (°)	α_{95} (°)
DDH47A/51	20	307.5	−10.5	9.0	307.5	−10.5	9.0
DDH42/44	21	292.2	−39.1	8.5	314.0	−4.7	5.8
TP*	19	308.8	−9.3	11.2	300.2	−16.0	14.7
PB*	15	304.7	−23.0	8.3	316.0	−6.9	8.7

Abbreviations: N = number of samples; D = declination; I = inclination; subscript h = with respect to present horizontal; subscript b = with respect to bedding (taking plunges into account), i.e. with respect to the palaeohorizontal; α_{95} = half-angle of Fisher's (1953) cone of confidence. DDH = diamond drill hole samples from depths greater than 50 m; 47A and 51 are from flat-lying BIFs at Wittenoom while 42 and 44 are from south-dipping BIFs at Paraburdoo; * = results marked thus are from iron ore and oxidized BIF samples near the surface.

tion but it is appropriate to emphasize here that had the magnetization postdated folding, the direction of remanence would be deflected towards the bedding. For some fold geometries this deflection would produce best grouping of directions from different fold limbs after a partial tilt correction. Thus the effects of anisotropy can in principle mimic the behaviour of syn-folding remanence. However, for these samples the best grouping occurs after complete unfolding, showing that the magnetization dates from before the time of folding. Further evidence that the palaeofield direction was close to the bedding plane is discussed in the next section.

5.5. *Effect of anisotropy on remanence directions*

The Hamersley BIFs consist of thin magnetite-rich bands separated by weakly magnetic layers. Self-demagnetization of the strongly magnetic layers produces a pronounced magnetic anisotropy, with a relatively isotropic plane of high susceptibility parallel to the banding and a substantially lower susceptibility normal to the banding. The magnetic anisotropy of the BIFs can therefore be characterized by a pure foliation, to a good approximation. The effect of the anisotropy is to deflect remanent magnetization away from the palaeofield direction, towards the bedding plane, producing a shallower apparent inclination and a lower apparent palaeolatitude.

Stacey and Banerjee (1974, pp. 83–84) have discussed the deflection of remanent magnetization in a strongly magnetic layer and McElhinny (1973, pp. 65–67) has analyzed the effect of anisotropy on remanence direction. More recently, Jackson (1991) has reviewed the various forms of magnetic anisotropy and methods for correction of measured remanence directions. We present a simple model, in order to allow correction of the measured directions for the effects of anisotropy and for self-demagnetization of the specimens.

Denote the intrinsic susceptibility of the magnetite-rich bands by χ, the corresponding CRM susceptibility (CRM intensity acquired in unit applied field) by χ_{CRM}, and the ARM susceptibility by χ_{ARM}. For simplicity, these intrinsic susceptibilities of the magnetite bands are assumed to be isotropic. In fact, there is a degree of preferred dimensional orientation of magnetite grains, with long axes lying within the bedding plane, and a tendency for magnetite grains to string together within bedding-parallel microbands. This will produce some intrinsic bedding-parallel magnetic foliation within the magnetite-rich bands, but intrinsic anisotropy of this type does not affect the following argument.

The SI demagnetizing factors of an extensive magnetic layer are 0, parallel to the layer, and 1, normal to the layer. It follows that the apparent susceptibility of each magnetite-rich band is χ, parallel to the bedding, and $\chi/(1+\chi)$, perpendicular to the bedding. If the magnetite-rich bands constitute fraction f of the total volume of a BIF unit, the effective bedding-parallel suscep-

tibility, $k_=$, and bedding-normal susceptibility, $k_\perp$, of the BIF are therefore:

$$k_= = f\chi$$

$$k_\perp = f\chi/(1+\chi)$$

Thus the susceptibility anisotropy, A, of the BIF unit is:

$$A = k_=/k_\perp = 1+\chi$$

Similarly, the CRM susceptibilities parallel to and normal to bedding and the anisotropy of CRM acquisition are:

$$(k_{CRM})_= = f\chi_{CRM}$$

$$(k_{CRM})_\perp = f\chi_{CRM}/(1+\chi_{CRM})$$

$$A_{CRM} = (k_{CRM})_=/(k_{CRM})_\perp = 1+\chi_{CRM}$$

Denote the palaeofield by F and the CRM vector by $\boldsymbol{M}$. If the palaeofield inclination at the time of primary CRM acquisition by a horizontal BIF unit is I, the inclination of the CRM is given by:

$$\tan(I_{CRM}) = \boldsymbol{M}_\perp/\boldsymbol{M}_= = (k_{CRM})_\perp F_\perp/(k_{CRM})_= F_=$$

$$\therefore \tan(I_{CRM}) = (1/A_{CRM})\tan I$$

Because $A_{CRM} > 1$, the CRM inclination of the BIF unit is lower than the palaeofield inclination. Determination of the palaeofield direction from the CRM direction requires an estimate of A_{CRM}.

Magnetic property measurements are carried out on standard cylindrical palaeomagnetic specimens, with dimensions chosen to best approximate spherical shape. Because the susceptibility of the specimens is high, the measured properties are affected by self-demagnetization. The demagnetizing factor for homogeneous quasispherical specimens is 1/3 and is isotropic. The apparent susceptibilities parallel and normal to bedding are therefore:

$$k'_= = k_=/(1+k_=/3)$$

$$k'_\perp = k_\perp/(1+k_\perp/3)$$

Thus the apparent anisotropy of the specimens is:

$$A' = k'_=/k'_\perp = A(1+k_\perp/3)/(1+k_=/3)$$

In the above, it is assumed that the banding occurs on a fine scale relative to the size of the specimen, so that the rock can be regarded as an essentially homogeneous, but anisotropic, medium on the specimen scale. This criterion was satisfied for the specimens used in this study, which contained many magnetite bands with typical thickness of ~ 1 mm.

Measurement of remanent magnetization is also affected by self-demagnetization. In other words, the effective magnetization of a sample, taken from a homogeneous strongly magnetic unit and placed in a zero field for determination of its remanence, depends on the sample shape. For homogeneous quasispherical specimens in a zero applied field the demagnetizing field arising from the net specimen magnetization $\boldsymbol{M}'$ is $-\boldsymbol{M}'/3$. This demagnetizing field induces a magnetization that opposes the remanence. If the in-situ remanent magnetization of the BIF unit is $\boldsymbol{M}$, then the specimen magnetization and the BIF remanence are related by:

$$(\boldsymbol{M}')_= = \boldsymbol{M}_= - k_=(\boldsymbol{M}')_=/3$$

$$(\boldsymbol{M}')_\perp = \boldsymbol{M}_\perp - k_\perp(\boldsymbol{M}')_\perp/3$$

$$\therefore (\boldsymbol{M}')_= = \boldsymbol{M}_=/(1+k_=/3)$$

$$(\boldsymbol{M}')_\perp = \boldsymbol{M}_\perp/(1+k_\perp/3)$$

Thus remanent magnetization of a specimen is reduced relative to the remanence of the rock unit by the same self-shielding factor, $(1+k/3)^{-1}$, as is the specimen susceptibility. Because the specimen susceptibility is anisotropic, the effect of self-demagnetization is anisotropic and the measured remanence inclination I'_{CRM} therefore differs from the remanence inclination recorded by the rock unit:

$$\tan(I'_{CRM}) = (\boldsymbol{M}')_\perp/(\boldsymbol{M}')_= = \tan(I_{CRM})(1+k_=/3)/(1+k_\perp/3)$$

The anisotropy of CRM acquisition for the specimen is:

$$A'_{CRM} = A_{CRM}(1+k_\perp/3)/(1+k_=)$$

$$\therefore \tan(I'_{CRM}) = (1/A'_{CRM})\tan I$$

Thus the magnetizations recorded by the BIFs are shallower than the prevailing palaeomagnetic field, but the *measured* magnetizations are somewhat steeper than the magnetizations of the rock unit (because the demagnetization factor within the bedding plane for the specimen shape is significant), partially correcting for the original deflection.

The palaeofield inclination can be simply calculated from the measured remanence inclination if A'_{CRM} is known. In practice, it is not possible to measure A'_{CRM}, but analogous quantities for thermoremanent magnetization (TRM), isothermal remanent magnetization (IRM) and anhysteretic remanent magnetization (ARM) can be readily determined. Of these, ARM is the closest analogue of CRM, because both magnetizations are acquired through equilibration of domain structure with the static applied field at ambient temperature. On the other hand, TRM involves equilibration at the blocking temperature, followed by cooling from the blocking temperature to room temperature with concomitant change in the magnetization. The analogy between IRM and CRM is less obvious, particularly since IRM is not linear in the applied field and IRM "susceptibility" cannot be rigorously described by a second-order tensor.

Stacey and Banerjee (1974) present simple phenomenological theories for multidomain CRM and ARM acquisition. Comparing their equations (9.18) and (10.4), it is evident that $\chi_{CRM} \approx \chi_{ARM}$ for multidomain magnetite. It follows from the discussion above that $A'_{CRM} \approx A'_{ARM}$. Thus ARM should serve as a satisfactory proxy for CRM for correction of the measured remanence inclinations. ARM anisotropies of selected specimens were determined by imparting ARMs in a static field of 0.1 mT with a peak alternating field of 100 mT. ARM was imparted successively along three orthogonal axes of each specimen and the ARM susceptibility tensor was calculated from the components of the ARM vectors. Before imparting an ARM along a new direction the specimen was AF demagnetized at 100 mT to erase any orthogonal ARM components. The NRM remaining after 100 mT demagnetization was subtracted from each measurement of ARM. The ARM susceptibility tensors were well defined using this method because of the high anisotropies. For each specimen the orientations of the principal axes of the susceptibility tensor and the ARM susceptibility tensor were almost identical, although the anisotropy ratios were greater for ARM susceptibility. As expected, the ARM magnetic fabric was highly oblate, with an almost isotropic plane of high ARM susceptibility parallel to bedding and a substantially lower ARM susceptibility normal to bedding.

The mean susceptibility tensor for 23 BIF specimens (comprising 13 specimens from the Dales Gorge Member, 6 from the Joffre Member and 4 from the Weeli Wolli Formation) corresponds to $k'_{=}=0.66$, $k'_{\perp}=0.35$, $A'=1.87$. The corresponding intrinsic anisotropy is $A=2.1$. Five specimens with thin, homogeneously distributed banding were chosen for determination of ARM anisotropy. The mean apparent susceptibilities for these specimens were $k'_{=}=0.98$, $k'_{\perp}=0.58$, corresponding to $A'=1.69$ and $A=2.0$. Thus these specimens have somewhat higher susceptibilities than average, but the intrinsic anisotropies are similar to the average value for the whole collection. The apparent ARM anisotropies ranged from 3.0 to 5.0, with a mean value for A'_{ARM} of 3.8.

Correcting the cleaned remanence inclinations for each specimen using this value of A'_{ARM} changes the mean direction for the Paraburdoo BIFs from $\bar{D}=313°$, $\bar{I}=-5°$ to $\bar{D}=313°$, $\bar{I}=-14°$. The corresponding palaeolatitude increases from 2.5° to 7.1°. Thus the effect of the anisotropy correction on the calculated palaeopole position is small, because of the low palaeolatitude at the time of remanence acquisition. The correction would be quite large, however, for remanence acquired at moderate palaeolatitudes. For example, a palaeolatitude of 30°, corresponding to a palaeofield inclination of 49°, would correspond to a measured remanence inclination of 17° and an apparent palaeolatitude of only 9°. The greatest discrepancy between apparent and true palaeolatitudes for this magnitude of anisotropy occurs for $\lambda=63°$ ($I=76°$),

which corresponds to a measured inclination of 46° and an apparent palaeolatitude of 27°. For very high palaeolatitudes the error again becomes negligible, because the magnetization component in the bedding plane is sufficiently small that the recorded magnetization is still steep, even after reduction of the normal component by self-demagnetization.

The cleaned remanence directions with respect to the palaeohorizontal, before and after correction for anisotropy, are shown in Fig. 10. Note that the spread in declinations of the subhorizontal uncorrected directions in Fig. 10a exceeds the spread in inclinations, so that the distribution of directions is not radially symmetric about the mean direction and hence is not Fisherian. This can be attributed to the anisotropy-induced flattening of the measured inclinations. On the other hand, the anisotropy-corrected directions in Fig. 10b show a greater spread in inclinations than in declinations, suggesting that they may have been overcorrected. Alternatively, the elongated distribution of corrected directions in the vertical plane may reflect apparent polar wander during a prolonged acquisition of remanence.

Because the range of inclinations is suppressed somewhat by the anisotropy, the α_{95} (6.1°) of the mean direction is underestimated when specimen directions are uncorrected for anisotropy. On the other hand, the α_{95} for the mean of the anisotropy-corrected directions is 12.6°, which is an overestimate of the true error because the spread in inclinations has been exaggerated by overcorrection for anisotropy, whereas the spread in declinations has been unaffected by the correction. Thus α_{95} for the approximately Fisherian distribution of directions centred on the true palaeofield direction should lie between 6.1° and 12.6°, suggesting that a reasonable estimate of the uncertainty of the mean direction is $\alpha_{95} \approx 9°$.

If the CRM anisotropy is somewhat smaller than the assumed value, which is based on ARM anisotropy, a more compact, circularly symmetric distribution of corrected directions would result. It seems likely that ARM anisotropy represents an upper limit to the value of CRM

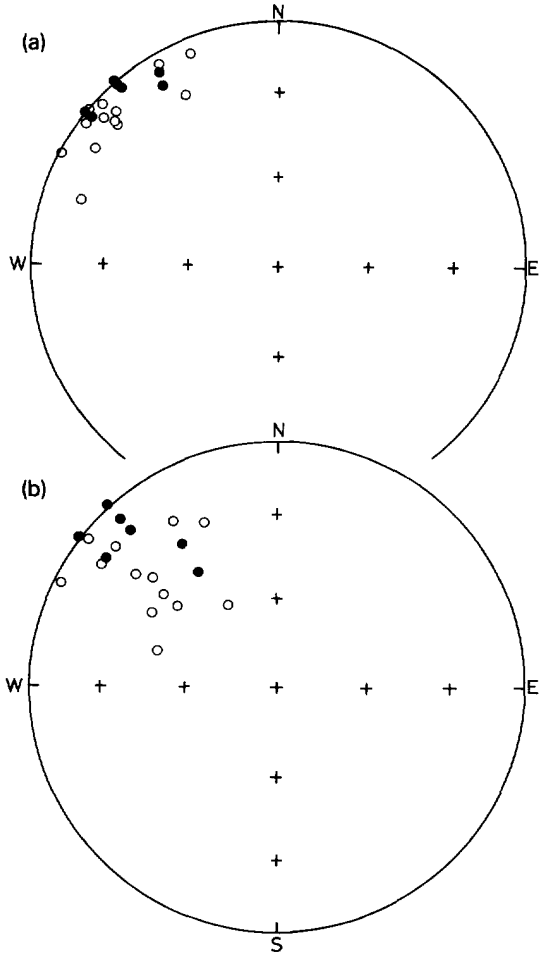

Fig. 10. Equal-area stereonet showing: (a) cleaned bedding corrected magnetization directions from BIF at Paraburdoo as measured (note some inclinations are positive and the distribution is flattened); and (b) same directions as (a) but corrected for anisotropy using anisotropy of ARM as an analogue for anisotropy of CRM (note this overcorrects and smears the distribution vertically). Conventions as for Fig. 6.

anisotropy. The effect of the alternating field is to assist domain wall motion over local energy barriers, whereas during CRM acquisition equilibration of domain structure with the internal field of magnetite grains may be hindered by pinning of the walls. Thus the intrinsic ARM susceptibility is expected to be somewhat higher than the intrinsic CRM susceptibility and therefore the ARM anisotropy of magnetite bands

should be higher than the CRM anisotropy. This expectation is supported by analysis of experimental data on field dependence of ARM susceptibility, which show that for weak-field ARM the effective susceptibility in the self-shielding factor $1/(1+N\chi)$ is about 2/3 of the intrinsic initial susceptibility, increasing to comparable values for static fields of ~5 mT (Stacey and Banerjee, 1974, pp. 141–145). As a result, ARM susceptibility given by Stacey and Banerjee's eq. (10.4) is somewhat higher than the CRM susceptibility given by their eq. (9.18).

Thus the errors in palaeoinclination and inferred palaeolatitude due to anisotropy are probably even less than estimated above, and can in this case be regarded as negligible in the context of the accuracy of the palaeomagnetic method. Additional evidence that the remanence carried by the BIFs was acquired in a subhorizontal palaeofield comes from the presence of both positive and negative inclinations in Fig. 10. Of the 21 directions, 5 have low positive inclinations and 3 are horizontal. This implies that the spread of inclinations recorded by these rocks straddles the palaeohorizontal, which is consistent with a shallow palaeofield. Furthermore, if the effects of anisotropy were larger than assumed here, the directions with positive and negative inclinations would scatter into widely separated groups on correction. As discussed in the section on tilt correction of remanence directions, the pre-folding signature, with no apparent syn-folding character, is further evidence that the deflection of remanence due to anisotropy is minor.

5.6. *Tilt correction of remanence directions from ore samples*

The remanence directions from the Tom Price and Paraburdoo ore samples show an increased scatter after structural correction, suggesting that the magnetization may be post-folding (Table 1). However, the increased dispersion of the Paraburdoo directions is slight, because of the small difference in structural attitudes of the sampled beds, and the fold test is not statistically significant. Thus it is not clear from the remanence directions whether the magnetization of the Paraburdoo ore predates or postdates the folding. Stratigraphic evidence indicates, however, that ore formation postdates the initial deformation of the Mount Bruce Supergroup. The similarity of the directions with the pre-folding directions from the BIFs suggests that the ore formation did not postdate the BIF greatly. This suggests that the magnetization of the BIFs is associated with burial metamorphism at the end of Turee Group time, immediately preceding folding, and the magnetization of the Paraburdoo ore records supergene enrichment soon after the folding and uplift of the Mount Bruce Supergroup.

The increase in dispersion of the Tom Price directions after untilting suggests that the Tom Price ore was magnetized after folding, although again the fold test is inconclusive. The directions isolated in this study are indistinguishable from the Paraburdoo ore directions but are, however, quite different from those found previously at Tom Price by Porath and Chamalaun (1968). This may be due to a combination of our sampling of a deeper level in the orebody, and a changing geomagnetic field during the ore-forming process. If we assume that the northwest upward directions found here represent normal polarity, then the samples collected for this study were magnetized in low southern hemisphere latitudes, while those collected by Porath and Chamalaun (1968) appear to have been magnetized in northern hemisphere latitudes. The secondary haematite-forming process at Tom Price appears to have spanned a greater length of time than it did at Paraburdoo, with the portion of the orebody sampled by us recording essentially the same event as at Paraburdoo, whereas the portion sampled by Porath and Chamalaun has recorded a different, presumably much later, event.

Without further sampling it is not possible to determine whether the palaeomagnetic results reflect two discrete episodes of haematite formation or, at the other extreme, very prolonged, essentially continuous, formation of haematite at Tom Price. The presence of both magnetic polarities in the Tom Price ore samples of this study, in contrast to the single polarity recorded by Paraburdoo ore, suggests that haematite formation

within the sampled portions of the orebodies was more prolonged at Tom Price than at Paraburdoo. During acquisition of the magnetization of the Tom Price ore, the Hamersley Basin appears to have moved through about 30° of latitude. The mean direction quoted by Porath and Chamalaun (1968) is $D=304°, I=25°$ ($\alpha_{95}=12°$) which is significantly different from the direction determined here (Table 1). The large dispersion of the Tom Price directions relative to other results in this study (Table 1 and from Mount Newman in Porath and Chamalaun, 1968) may be attributed, in part, to continental drift although the presence of both polarities is possibly also instrumental. The palaeomagnetic signature of the ore may also have been somewhat disrupted by leaching of goethite and consequent volume loss during the Mesozoic/Tertiary. One possible interpretation is that the magnetization found in this study records the early supergene enrichment stage of martite–goethite ore formation, as at Paraburdoo, and the magnetization found by Porath and Chamalaun (1968) records the later formation of microplaty haematite during burial of the martite–goethite ore.

The mean direction quoted by Porath and Chamalaun (1968) from Mount Newman is $D=302°, I=39°$ ($\alpha_{95}=10°$). This result is supported by the results from samples collected for this study, which yield a direction of $D=308°, I=50°$ ($\alpha_{95}=8°$), indicating magnetization in mid-northern latitudes (on the basis of the previously assumed hemisphere convention). There is no indication of the presence of magnetic reversals at Mount Newman, suggesting that the magnetization acquisition there was of relatively short duration. The magnetization direction recorded by the Mount Newman orebody is almost identical to that detected in the Tom Price orebody by Porath and Chamalaun (1968), suggesting that ores at these two localities have recorded the same event, probably formation of microplaty haematite. The high unblocking temperatures of the haematite that carries the characteristic remanence of the iron ores imply that, once formed, the magnetization of the ores could not have been overprinted by later thermal events, unless temperatures far higher than ever prevailed in the Hamersley Basin had been attained.

6. Discussion and conclusions

The Hamersley BIFs and iron ore formations have yielded reliable Palaeoproterozoic palaeomagnetic directions and palaeomagnetic pole positions. From the anisotropy of ARM a 9° deflection of the magnetic inclination of the BIFs is suggested, although this is an overestimate of the actual CRM anisotropy. However, the calculated pole position is shifted less than 5°. The directions and pole positions are pre-folding for the BIFs but probably post-folding for the iron ores. These are: (i) for Wittenoom BIF, $D=307.5, I=-10.5$ ($\alpha_{95}=9.0$) and pole at 36.4°S, 218.9°E ($dp=4.6°$, $dm=9.1°$); (ii) for Paraburdoo BIF, $D=314.0, I=-4.7$ ($\alpha_{95}=5.8$) and pole at 40.9°S, 225.0°E ($dp=2.9°$, $dm=5.8°$); (iii) for Mount Tom Price iron ore, $D=308.8, I=-9.3$ ($\alpha_{95}=11.2$) and pole at 37.4°S, 220.3°E ($dp=5.7°$, $dm=11.3°$); and (iv) Paraburdoo iron ore, $D=304.7, I=-23.0$ ($\alpha_{95}=8.3$) with pole at 36.4°S, 209.9°E ($dp=4.7°$, $dm=8.8°$).

The implications of palaeomagnetic results are most conveniently considered in terms of an apparent polar wander path (APWP). The Precambrian APWP for Australia is only rudimentarily known, and is based on combining results from different cratons. This procedure implicitly assumes that the cratons have not moved greatly with respect to each other since the time of interest. Poles from the different cratons appear to form a reasonably simple APWP which has been seen as support for this assumption (McElhinny and Embleton, 1976). In a discussion of the Australian Precambrian data, Idnurm and Giddings (1988) point out that the average pole density is one per sixty million years. This, plus the "polarity option", prevents the Australian APWP from being uniquely defined. However, there is a relatively high number of Early Precambrian results from within the Pilbara Craton itself, so it is considered worthwhile

to examine the results in terms of APWP (Fig. 11).

Poles PB and TP2 from the iron ores studied here, and TP1 and MN from the iron ores studied by Porath and Chamalaun (1968) are spread over 30° of longitude and suggest that some APWP has occurred during iron ore formation. The close proximity of the BIF poles and the PB and TP2 pole is also notable. Because the BIF poles represent pre-folding magnetizations, whereas iron ores formed after folding, the data indicate a surprisingly small amount of APW for the period between acquisition of BIF magnetization and iron ore formation. This suggests that the BIF magnetization was acquired soon before folding, and the PB and TP2 magnetizations soon after. The BIF magnetization is attributable to CRM acquired during formation of magnetite from primary haematite due to burial metamorphism, probably in latest Turee Group time. The Mount Jope Volcanics overprint magnetization is syn-folding and the corresponding pole (JO) is essentially coincident with the BIF pole, again suggesting that the BIF magnetization is not much older than the deformation. The age of these magnetizations is not well constrained, but on the basis of reasonable assumptions about deposition rates Trendall (1983) suggests that the top of the Turee Group could be as old as ~2300 Ma. Morris (1985) suggests 2000±200 Ma as the age of the supergene enrichment event that produced the martite–goethite ores. The palaeomagnetic evidence suggests that the sequence of events: (i) peak of burial metamorphism and ac-

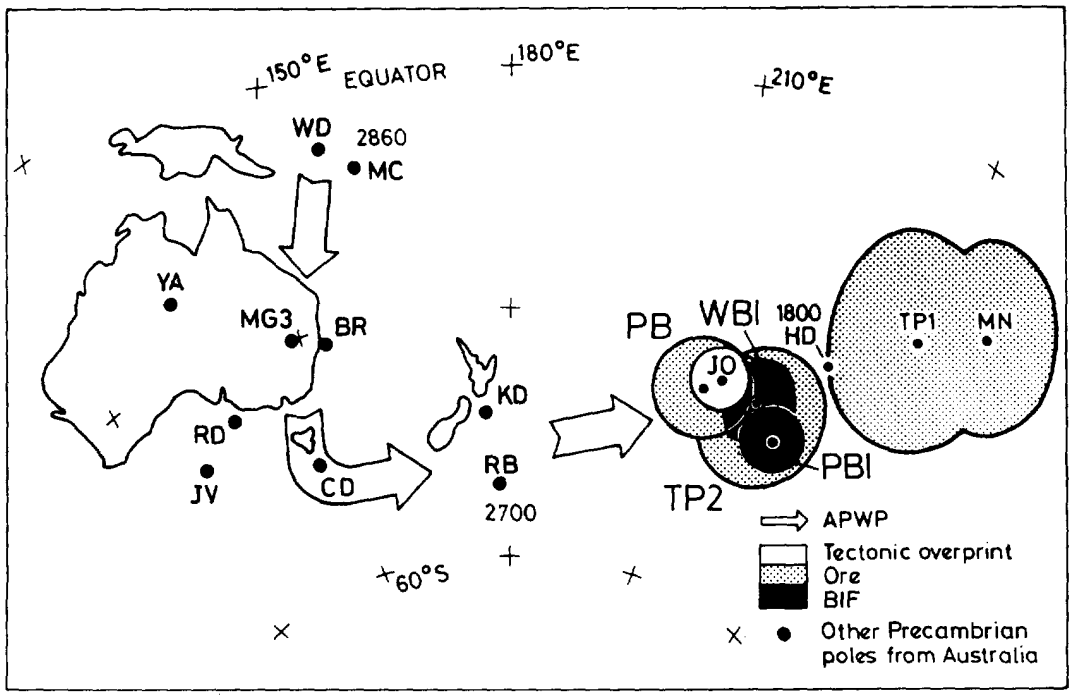

Fig. 11. APWP showing poles from this study and related poles. Pole mnemonics are: *PBI* and *WBI*, Paraburdoo and Wittenoom banded-iron formations (BIFs), respectively; *PB* and *TP2*, Paraburdoo and Mount Tom Price iron ore/oxidized BIF, respectively. Other mnemonics are those used by Idnurm and Giddings (1988): *WD*=Widgiemooltha dyke (Evans, 1968); *MIL*=Millindinna Complex; *JV*=Mount Jope Volcanics; *RB*=Mount Roe Basalt and *JO*=Mount Jope Volcanics syn-folding overprint (Schmidt and Embleton, 1985); *YA*=Yilgarn A dykes and *RD*=Ravensthorpe dyke (Giddings, 1976); *MG3*=Mount Goldsworthy 3; *KD*=Koolyanobbing Dowd's Hill; *TP1*=Mount Tom Price iron ore and *MN*=Mount Newman iron ore (Porath and Chamalaun, 1968); *BR*=Black Range dyke and *CD*=Cajuput dyke (Embleton, 1978); *HD*=Hart Dolerite (McElhinny and Evans, 1976).

quisition of BIF CRM, (ii) folding and uplift, and (iii) supergene enrichment, was relatively rapid, unless APW was anomalously slow at this time or the apparently identical poles are in fact of opposite polarity. This latter possibility requires 180° of APW between acquisition of BIF and ore magnetizations, which coincidentally recorded identical orientations of the geomagnetic dipole axis.

In fact, Idnurm and Giddings (1988) indicate approximately 180° of polar wander between the 2500 Ma and 1800 Ma segments of their pole path. However, Idnurm and Giddings (1988) do admit that the pole YF (their fig. 3), which is the cornerstone of this option, is poorly controlled in age. Also, it should be noted that the new BIF pole does not fall on the Idnurm and Giddings path, which would require considerable modification to incorporate the pole, unless the BIF magnetization was acquired as late as ~1900 Ma. This seems implausible, however, given the time required for deformation, uplift and erosion of the Mount Bruce Supergroup, deposition of the Lower Wyloo Group, further deformation, uplift and erosion, and deposition of part of the Upper Wyloo Group, all before ~1850 Ma. Thus modifying the Idnurm and Giddings path to pass through the BIF pole would require a remarkable coincidence of the dipole axis, returning to its previous location after traversing the globe from ~2300 Ma to ~1900 Ma ago. On balance this suggests that perhaps the short path used here (and used in the past by various workers) is more plausible.

Development of the PB ore appears to have been arrested relative to TP and MN ores, leaving it with a magnetization somewhat older than many ores at TP and MN. Similarly to the TP and MN ores, the PB ore shows no palaeomagnetic evidence for Neoproterozoic or Phanerozoic modification.

Our preferred interpretation, which we believe to be the most parsimonious explanation of the palaeomagnetic data, consistent with geological constraints, consists of the following elements.

(i) The magnetization of the BIFs is associated with replacement of primary haematite with magnetite during burial metamorphism and was acquired relatively late, during latest Turee Group time, immediately before folding of the Mount Bruce Supergroup. The age of BIF magnetization is estimated to be 2200 ± 100 Ma.

(ii) The magnetization of Paraburdoo ore and part of the Tom Price orebody records supergene enrichment of fresh BIF to produce martite–goethite ore relatively soon after the main folding of the Mount Bruce Supergroup, at about 2000 ± 100 Ma.

(iii) The Mount Newman orebody records formation of microplaty haematite ore, following reburial of martite–goethite ore, at about 1950 ± 100 Ma. The Tom Price orebody exhibits a more complex magnetization history than at the other two mines, apparently retaining a more complete record of the prolonged ore-forming process. Both the initial supergene enrichment and the replacement of goethite by microplaty haematite are recorded by the Tom Price orebody.

A puzzling feature of these data is the apparent simplicity of the magnetization carried by the Paraburdoo ore, which appears to be close in age to the BIF magnetization and which is best interpreted as CRM acquired early in the ore-forming process, during the supergene enrichment phase. It is unclear why the substantial replacement of goethite by microplaty haematite during subsequent burial has apparently not been recorded palaeomagnetically. At Mount Newman, on the other hand, the apparent absence of a remanence component carried by martite, and inherited from the supergene enrichment phase, has not been explained. Perhaps extensive development of microplaty haematite can mechanically disrupt pre-existing martite grains, randomizing their orientations and destroying their palaeomagnetic information. If this occurred at Mount Newman and in part of the Tom Price orebody, why was the Paraburdoo remanence not similarly reset when the microplaty haematite was forming? Answers to these questions await further research. In particular, there is a requirement for studies that relate the detailed mineralogy and geology of different ore types to their magnetizations, in order to elucidate the rela-

tionships between palaeomagnetism and geological events in this complex and fascinating geological environment.

The techniques applied and developed in this paper have considerable potential for extending palaeomagnetic studies to other BIFs, and to anisotropic rocks in general. Combined mineralogical and palaeomagnetic studies of iron ores also have potential for elucidating iron ore genesis and for filling some of the vast gaps in the Precambrian palaeomagnetic record.

Acknowledgements

The authors are grateful for assistance from and discussions with many people during the course of this study. These include Bob Smith of CRA Exploration Ltd. and Bill Burns of Hamersley Exploration Ltd. Dick Morris (CSIRO) explained in great detail the mineralogical character of the various iron ores and geological constraints on the ore-forming processes. John Ashley and Peter de Groot are thanked for discussions on interpretation of magnetic surveys in the Hamersley Basin. Alex Mandyczewsky and Richard Harmsworth were very proficient guides in the field. This paper was improved by Mart Idnurm's careful review.

References

Arndt, N.T., Nelson, D.R., Compston, W., Trendall, A.F. and Thorne, A.M., 1991. The age of the Fortescue Group, Hamersley Basin, Western Australia, from ion microprobe zircon U–Pb results. Aust. J. Earth Sci., 38: 261–281.

Blockley, J.G., 1990. Iron ore. In: Geology and Mineral Resources of Western Australia. Geol. Surv. W. Aust., Mem., 3: 679–692.

Chamalaun, F.H. and Dempsey, C.E., 1978. A survey of the magnetic properties of the banded iron formations, Hamersley Province. W. Aust. Dep. Earth Sci., Flinders Univ. Publ., 78/4: 51.

Cloud, P., 1983. Banded-iron formation—a gradualist's dilemma. In: A.F. Trendall and R.C. Morris (Editors), Banded-Iron Formations: Facts and Problems. Elsevier, Amsterdam, pp. 401–416.

Collinson, D.W., 1983. Methods in Rock Magnetism and Palaeomagnetism, Techniques and Instrumentation. Chapman and Hall, London, 503 pp.

Compston, W., Williams, I.S., McCulloch, M.T., Foster, J.J., Arriens, P.A. and Trendall, A.F., 1981. A revised age for the Hamersley Group. Geol. Soc. Aust., 5th Annu. Convention, Perth, Abstr., 3: 40.

Embleton, B.J.J., 1978. The palaeomagnetism of 2400 m.y. old rocks from the Australian Pilbara Craton and its relation to Archaean–Proterozoic tectonics. Precambrian Res., 6: 275–291.

Embleton, B.J.J., Robertson, W.A. and Schmidt, P.W., 1979. A survey of magnetic properties of some rocks from northwestern Australia. Investigation Report 129, CSIRO, Division of Mineral Physics, North Ryde, Sydney.

Evans, M.E., 1968. Magnetization of dykes: a study of the palaeomagnetism of the Widgiemooltha Dike Suite, Western Australia. J. Geophys. Res., 73: 3261–3270.

Ewers, W.E. and Morris, R.C., 1981. Studies of the Dales Gorge Member of the Brockman Iron Formation, Western Australia. Econ. Geol., 76: 1929–1953.

Giddings, J.W., 1976. Precambrian palaeomagnetism in Australia, I. Basic dykes and volcanics from the Yilgarn Block. Tectonophysics, 30: 91–108.

Graham, J.W., 1949. The stability and significance of magnetism in sedimentary rocks. J. Geophys. Res., 54: 131–167.

Harmsworth, R.A., Kneeshaw, M., Morris, R.C., Robinson, C.J. and Shrivastsava, P.K., 1990. BIF-derived iron ores of the Hamersley Province. In: F.E. Hughes (Editor), Geology of the Mineral Deposits of Australia and Papua New Guinea. Australian Institute of Mining and Metallurgy, Melbourne, Monogr. 14, pp. 617–642.

Hassler, S.W., 1993. Depositional history of the Main Tuff Interval of the Wittenoom Formation, late Archaean–early Proterozoic Hamersley Group, Western Australia. Precambrian Res., 60: 337–359.

Horwitz, R.C., 1983. Palaeogeographic evolution of the Paraburdoo Hinge Zone: a summary of events. In: W.E. Ewers (Editor), Research Review. CSIRO Division of Mineralogy, Floreat Park, Perth.

Hrouda, F., Stephenson, A. and Woltar, L., 1983. On the standardization of measurements of anisotropy of magnetic susceptibility. Phys. Earth Planet. Inter., 32: 203–208.

Idnurm, M. and Giddings, J.W., 1988. Australian Precambrian polar wander: a review. Precambrian Res., 40/41: 61–88.

Idnurm, M. and Schmidt, P.W., 1986. Palaeomagnetic dating of weathered profiles. Geol. Surv. India Mem., 120: 79–88.

Idnurm, M. and Senior, B.R., 1978. Palaeomagnetic ages of Late Cretaceous and Tertiary weathering profiles of the Eromanga Basin, Queensland. Palaeogeogr., Palaeoecol., Palaeoclimatol., 24: 263–272.

Jackson, M., 1991. Anisotropy of magnetic remanence: a brief review of mineralogical sources, physical origins, and

geological applications, and comparison with susceptibility anisotropy. Pageoph, 136: 1–28.

Klein, C., 1983. Diagenesis and metamorphism of Precambrian banded-iron formations. In: A.F. Trendall and R.C. Morris (Editors), Iron-Formation: Facts and Problems. Developments in Precambrian Geology 6, Elsevier, Amsterdam, pp. 417–469.

Koenigsberger, J.G., 1938. Natural residual magnetism in eruptive rocks, parts I and II. Terr. Magn. Atmos. Electr., 43: 119–127 and 299–320.

Leggo, P.J., Compston, W. and Trendall, A.F., 1965. Radiometric ages of some Precambrian rocks from the Northwest Division of Western Australia. J. Geol. Soc. Aust., 12: 53–65.

McElhinny, M.W., 1973. Palaeomagnetism and Plate Tectonics. Cambridge University Press, Cambridge, 358 pp.

McElhinny, M.W. and Embleton, B.J.J., 1976. Precambrian and early Palaeozoic palaeomagnetism in Australia. Philos. Trans. R. Soc. London, Ser. A, 280: 417–431.

McElhinny, M.W. and Evans, M.E., 1976. Palaeomagnetic results from the Hart Dolerite of the Kimberley Block, Australia. Precambrian Res., 3: 231–241.

McFadden, P.L. and Jones, D.L., 1981. The fold test in palaeomagnetism. Geophys. J. R. Astron. Soc., 67: 53–58.

Morris, R.C., 1980. A textural and mineralogical study of the relationship of iron ore to banded-iron formation in the Hamersley Iron Province of Western Australia. Econ. Geol., 75: 184–209.

Morris, R.C., 1983. Supergene alteration of banded-iron formation. In: A.F. Trendall and R.C. Morris (Editors), Iron-Formation: Facts and Problems. Developments in Precambrian Geology 6, Elsevier, Amsterdam, pp. 513–534.

Morris, R.C., 1985. Genesis of iron ore in banded-iron formation by supergene and supergene-metamorphic processes—a conceptual model. In: K.H. Wolf (Editor), Handbook of Strata-Bound and Stratiform Ore Deposits 13, Elsevier, Amsterdam, pp. 73–235.

Pidgeon, R.T. and Horwitz, R.C., 1991. The origin of olistoliths in Proterozoic rocks of the Ashburton Trough, Western Australia, using zircon U–Pb isotopic characteristics. Aust. J. Earth Sci., 38: 55–63.

Porath, H. and Chamalaun, F.H., 1968. Palaeomagnetism of Australian haematite ore bodies, II. Western Australia. Geophys. J. R. Astron. Soc., 15: 253–264.

Ridley, B.H. and Brown, H.E., 1980. The transformer bridge and magnetic susceptibility measurements. Bull. Aust. Soc. Explor. Geophys., 11: 110–114.

Roy, J.L., Reynolds, J. and Sanders, E., 1973. An alternating field demagnetizer for rock magnetism studies. Publ. Earth Phys. Branch, 44-3: 37–45.

Schmidt, P.W., 1982. Linearity spectrum analysis of multicomponent magnetizations and its application to some igneous rocks from south-eastern Australia. Geophys. J. R. Astron. Soc., 79: 647–665.

Schmidt, P.W. and Embleton, B.J.J., 1976. Palaeomagnetic results from sediments of the Perth Basin, Western Australia, and their bearing on the timing of regional lateritization. Palaeogeogr., Palaeoecol., Palaeoclimatol., 19: 257–273.

Schmidt, P.W. and Embleton, B.J.J., 1985. Pre-folding and overprint magnetic signatures in Precambrian (~2.9–2.7 Ga) igneous rocks from the Pilbara Craton and Hamersley Basin, N.W. Australia. J. Geophys. Res., 90: 2967–2984.

Smith, R.E., Perdrix, J.L. and Parks, T.C., 1982. Burial metamorphism in the Hamersley Basin, Western Australia. J. Petrol., 23: 75–102.

Stacey, F.D. and Banerjee, S.K., 1974. The Physical Principles of Rock Magnetism. Elsevier, Amsterdam, 195 pp.

Trendall, A.F., 1983. The Hamersley Basin. In: A.F. Trendall and R.C. Morris (Editors), Iron-Formation: Facts and Problems. Developments in Precambrian Geology 6, Elsevier, Amsterdam, pp. 513–534.

Trendall, A.F., 1990. Hamersley Basin. In: Geology and Mineral Resources of Western Australia. Geol. Surv. W. Aust., Mem., 3: 163–189.

Trendall, A.F. and Blockley, J.G., 1970. The iron associations of the Precambrian Hamersley Group, Western Australia, with special reference to the associated crocidolite. W. Austr. Geol. Surv., Bull. 119, 336 pp.

Veitch, R.J., Hedley, I. and Wagner, J.-J., 1983. Magnetic anisotropy delineator calibration error. Geophys. J. R. Astron. Soc., 75: 407–409.

Zijderveld, J.D.A., 1967. A.C. demagnetization of rocks: analysis of results. In: D.W. Collinson, K.M. Creer and S.K. Runcorn (Editors), Methods in Palaeomagnetism. Elsevier, Amsterdam, pp. 254–286.